

Photoluminescence spectroscopy of bandgap reduction in dilute InNAs alloys

T. D. Veal, L. F. J. Piper, P. H. Jefferson, I. Mahboob,^{a)} and C. F. McConville^{b)}
Department of Physics, University of Warwick, Coventry CV4 7AL, United Kingdom

M. Merrick, T. J. C. Hosea, and B. N. Murdin
Advanced Technology Institute, School of Electronics and Physical Sciences, University of Surrey, Guildford GU2 7XH, United Kingdom

M. Hopkinson
Department of Electronic and Electrical Engineering, University of Sheffield, Mappin Street, Sheffield S1 3JD, United Kingdom

(Received 29 July 2005; accepted 27 September 2005; published online 28 October 2005)

Photoluminescence (PL) has been observed from dilute $\text{InN}_x\text{As}_{1-x}$ epilayers grown by molecular-beam epitaxy. The PL spectra unambiguously show band gap reduction with increasing N content. The variation of the PL spectra with temperature is indicative of carrier detrapping from localized to extended states as the temperature is increased. The redshift of the free exciton PL peak with increasing N content and temperature is reproduced by the band anticrossing model, implemented via a (5×5) $\mathbf{k} \cdot \mathbf{p}$ Hamiltonian. © 2005 American Institute of Physics.

[DOI: 10.1063/1.2126117]

In dilute nitrides, the substitution of highly electronegative nitrogen atoms for a few percent of the host anions in a III–V semiconductor results in the formation of a highly localized resonant band above the conduction band minimum (CBM).^{1,2} The localized interaction between the host conduction band and the narrow resonant level, formed by the nitrogen states, results in a large reduction of the band gap. This has been successfully described for a range of dilute nitrides, including GaNAs, GaInNAs, and InNP, by the band anticrossing (BAC) model.^{1–4} Due to this unusual property, dilute nitrides are recognized as having great potential for various device applications.^{3,4} While a great deal of attention has been paid to GaNAs and GaInNAs alloys for near-infrared applications, the investigation of related dilute nitride alloys, such as GaNSb (Ref. 5) and InNAs,^{6–9} for mid-infrared applications is only in its infancy. Indeed, band gap reduction has proved difficult to observe unambiguously in absorption spectra from InNAs alloys.^{7–9} The reduction of the absorption-edge energy with increasing nitrogen content has so far only been observed in one optical absorption study of InNAs alloys.⁶

Generally, absorption edges at higher energies than the true band gap are observed in n -type InNAs epilayers.^{7–9} This is due to the Moss-Burstein effect,^{10,11} resulting from band filling due to unintentionally degenerate n -type doping in the InNAs alloy. This proclivity of InAs and InNAs for n -type conductivity is consistent with the amphoteric defect model.¹² The formation of donor-like impurities and defects is favoured because the Γ -point CBM in InAs is below the branch-point energy, E_B .¹³ The incorporation of dilute amounts of nitrogen lowers the CBM further, making the tendency towards degenerate n -type conductivity even stronger in InNAs than in InAs. This increase of electron concentration with increasing nitrogen content has been observed

by Hall measurements of InNAs films grown on semi-insulating GaAs substrates by molecular-beam epitaxy (MBE).⁸ Therefore, the nitrogen-induced band gap reduction in InNAs can generally only be estimated from absorption spectroscopy once the contribution of Moss-Burstein shift to the position of the absorption edge has been modeled.^{7–9}

In this letter, the temperature dependence of photoluminescence (PL) from dilute InNAs films grown by MBE is reported. The PL spectra unambiguously show band gap reduction with increasing N content. For degenerate doping, optical absorption transitions can only occur for photon energies higher than the energy needed for electrons to make transitions from the valence band up to the Fermi level in the conduction band.¹⁴ By contrast, the PL peak is due to the photons spontaneously emitted when electrons from the conduction band recombine with holes in the valence band. As a result, PL measurements of the band gap are not significantly affected by moderately high Fermi levels in the conduction band. However, PL still has to be interpreted with caution, since at low temperatures it can originate from the tail of localized states at the band edge associated with any disorder in the alloy.¹⁵

The InNAs epilayers were coherently grown to a thickness of 300 nm on InAs(001) substrates by MBE using a turbopumped Vacuum Generators V80 system equipped with an Oxford Applied Research (OAR) HD25 rf plasma nitrogen source. The samples were all grown with a substrate temperature of 375 °C. The nitrogen incorporation in the InNAs samples was varied by changing the plasma power and nitrogen gas pressure. The nitrogen content was determined by x-ray diffraction (XRD) using $\text{Cu } K_\alpha$ ($\lambda = 1.5406 \text{ \AA}$) as the radiation source. XRD curves around the 004 Bragg reflections, recorded to measure the lattice constants of the epilayers, are shown in Fig. 1. The N contents, determined from the epilayer lattice constants assuming Vegard's law, are $x=0.010$, 0.022, and 0.028. The full width at half maxima (FWHM) of the epilayer XRD peaks are

^{a)}Present address: NTT Basic Research Laboratories, Morinosato Wakamiya, Atsugi-shi, Kanagawa 243-0198, Japan.

^{b)}Electronic mail: C.F.McConville@warwick.ac.uk

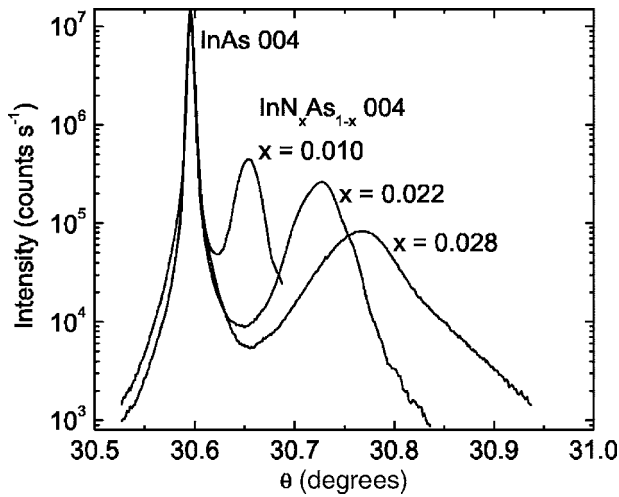


FIG. 1. X-ray diffraction of the 004 Bragg peaks from nominally 300-nm-thick InAs epilayers MBE-grown on InAs(001) substrates, indicating N contents of 1.0%, 2.2%, and 2.8%.

83, 145, and 253 arc sec for $x=0.010$, 0.022, and 0.028, respectively.

For the PL measurements, the samples were held in a liquid-nitrogen cryostat with CaF windows, and excited with a mechanically chopped, ~ 65 mW, $1.064 \mu\text{m}$, diode-pumped Nd:yttrium-aluminum-garnet laser (typical sample spot diameter ~ 2 mm). The spectra were analyzed with a Bomem midinfrared fast-scanning Fourier-transform infrared (FTIR) spectrometer, a liquid-nitrogen-cooled InSb detector and a digital lock-in amplifier. Since the maximum fringe modulation frequency of the FTIR spectrometer is ~ 3.3 kHz due to mirror scanning, it was necessary to chop the laser at the relatively high frequency of 20 kHz.

Photoluminescence spectra from InAs, $\text{InN}_{0.010}\text{As}_{0.990}$, and $\text{InN}_{0.022}\text{As}_{0.978}$ recorded at temperatures of between 78 and 293 K are shown in Fig. 2. The InAs PL peak broadens and shifts to lower energy as the temperature is increased. The PL peak from $\text{InN}_{0.010}\text{As}_{0.990}$ exhibits an initial shift to higher energy as the temperature is raised from 78 to 175 K,

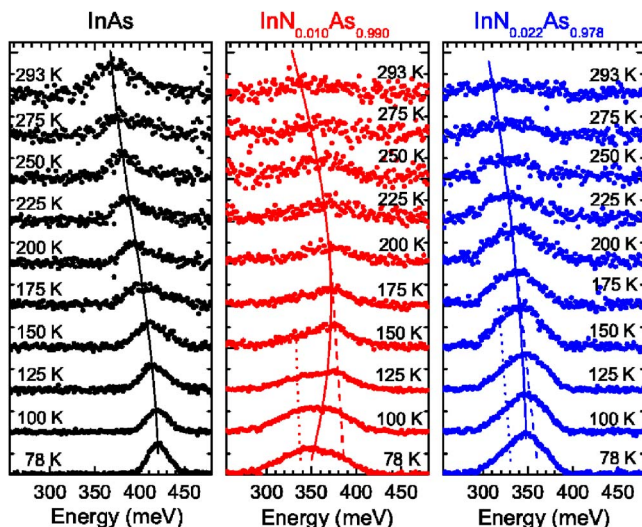


FIG. 2. (Color online) PL spectra recorded at temperatures between 78 and 293 K from InAs, $\text{InN}_{0.010}\text{As}_{0.990}$, and $\text{InN}_{0.022}\text{As}_{0.978}$ (with an arbitrary intensity scale). The solid lines follow the PL peak position, while the dashed and dotted lines indicate the positions of the free exciton and localized exciton peaks, respectively, in the PL spectra recorded below 175 K.

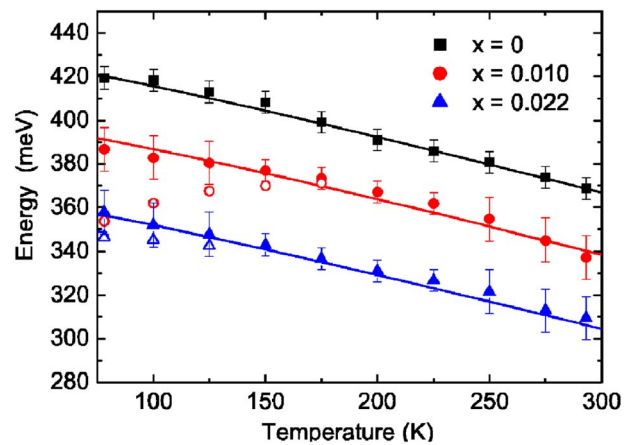


FIG. 3. (Color online) The temperature dependence of the PL spectra from InAs, $\text{InN}_{0.010}\text{As}_{0.990}$ and $\text{InN}_{0.022}\text{As}_{0.978}$. The solid symbols indicate the free exciton peak position. The open symbols depict the PL peak position, where this differs from that of the free exciton peak. The line through the InAs data points is from Varshni's relation for the temperature dependence of the band gap. The lines through the $\text{InN}_x\text{As}_{1-x}$ data points represent the temperature dependence of the band gap calculated using a $\mathbf{k}\cdot\mathbf{p}$ model of the interaction between the localized N-induced resonant states and the host conduction band.

followed by a shift to lower energy between 200 and 293 K. This blueshift followed by redshift is due to localization of electrons in potential fluctuations, originating from the random N distribution in the alloy.³ At low temperatures, the broad PL peak is composed of contributions from localized excitons (LE) and free excitons (FE). The variation of the PL spectra with increasing temperature is indicative of carrier detrapping from localized to extended states.¹⁶ As the temperature is increased, the PL peak initially narrows due to the reduction in the intensity of the LE peak with respect to the FE peak. The PL peak reaches its lowest FWHM at 175 K, before increasing again due to the thermalization of the carriers.¹⁷ Also above ~ 175 K, only the FE peak is present and the PL peak redshift is solely associated with the reduction of the band gap with increasing temperature.

The PL from the $\text{InN}_{0.022}\text{As}_{0.978}$ sample exhibits a similar trend to the lower N content, but with less separation between the LE and FE peaks. From the highest nitrogen content sample, $\text{InN}_{0.028}\text{As}_{0.972}$, only a weak PL peak originating from the InAs substrate was observed. The lack of PL from this alloy is attributed to the poorer crystal quality of this epilayer, as indicated by the broader XRD peak.

The position of the free exciton PL peak (closed symbols) as a function of temperature for each of the samples is plotted in Fig. 3, along with the PL peak position (open symbols) where this differs from that of the free exciton peak. At a given temperature, as the N content is increased the FE PL peak position decreases in energy. This provides unambiguous evidence of the N-induced band gap reduction in InNAs alloys. The line through the InAs data points is from Varshni's relation for the temperature dependence of the band gap,¹⁸ using $E_g(0)=430$ meV (while Vurgaftman *et al.* recommend the value $E_g(0)=417$ meV, they report that the literature values range from 410 to 450 meV) and the Varshni parameters $A=0.276$ meV/K and $B=93$ K.¹⁹ The lines through the $\text{InN}_x\text{As}_{1-x}$ data points represent the calculated temperature dependence of the band gap. This was calculated using a $\mathbf{k}\cdot\mathbf{p}$ model of the interaction of the extended Γ states of the host semiconductor conduction band with the

localized N-induced resonant states. This interaction results in the formation of two nonparabolic subbands E_+ and E_- , with the band gap then being the separation between the valence band maximum and the E_- subband minimum.

The evolution of the E_{\pm} subband edges with nitrogen content, x , can be determined by finding the eigenvalues of

$$\begin{vmatrix} E - E_N(x) & \beta x^{1/2} \\ \beta x^{1/2} & E - E_{c0} - \alpha x \end{vmatrix}, \quad (1)$$

where $\alpha=1.30$ eV (Ref. 20) is the parameter of the term describing the linear variation of the conduction band edge with N content, $\beta=1.30$ eV (Ref. 20) is the parameter of the term describing the interaction between the N resonant state and the conduction band edge, $E_N(x)$ is the effective N level with respect to the valence band maximum, and E_{c0} is the host conduction band edge.²¹ However, this becomes a 5×5 Hamiltonian when conventional $\mathbf{k} \cdot \mathbf{p}$ theory is included to account for the intrinsic nonparabolicity of the host InAs. The temperature dependence of the host band gap was described by the same Varshni parameters as used to produce the line through the InAs data points in Fig. 3. The change in the effective N level due to the increased concentration of N pairs with increasing x content is accounted for by $E_N(x)=E_{N0}-\gamma x$,¹⁵ where $E_{N0}=1.48$ eV is the isolated N resonant state and $\gamma=2.00$ eV.²⁰

The parameters for the $\mathbf{k} \cdot \mathbf{p}$ Hamiltonian were determined by fitting the resulting E_{\pm} subbands to the tight binding band structure of $\text{InN}_x\text{As}_{1-x}$. Details of the tight binding calculation can be found elsewhere.¹⁵ However, to fit the experimental variation of the FE PL peak, the value of E_{N0} had to be changed from the tight binding value of 1.36 eV. A value of 1.48 eV was used, in agreement with that obtained by Shih *et al.*⁷ Using the BAC model,¹ the experimental data are reproduced when the nitrogen level and coupling parameter have the values $E_{N0}=1.48$ eV (with $\gamma=2.00$ eV) and $C_{MN}=1.77$ eV, respectively. This value of C_{MN} is between those of 1.68 and 1.86 eV reported by Shih *et al.*⁷ and Kuroda *et al.*,⁸ respectively, obtained from fitting the N content dependence of the absorption edge after correcting for Moss-Burstein shift.

The dependence on temperature of the PL spectra indicates the presence of localized and free carriers. While both are present at low temperature, the latter dominate at high temperature. The band gap reduction induced by the incorporation of nitrogen in InNAs alloys is unambiguously observed by PL spectroscopy of the free exciton peak. The dependence of the band gap on nitrogen content and temperature has been modeled using five band $\mathbf{k} \cdot \mathbf{p}$ and the BAC model.

The authors would like to thank Andrew Lindsay and Eoin O'Reilly for providing the $\mathbf{k} \cdot \mathbf{p}$ parameters for InNAs from their tight binding calculations. The Engineering and Physical Sciences Research Council, UK is acknowledged for financial support under Grant No. GR/S56030/01.

¹W. Shan, W. Walukiewicz, J. W. Ager III, E. E. Haller, J. F. Geisz, D. J. Friedman, J. M. Olson, and S. R. Kurtz, Phys. Rev. Lett. **82**, 1221 (1999).

²J. Wu, W. Shan, and W. Walukiewicz, Semicond. Sci. Technol. **17**, 860 (2002).

³*Physics and Applications of Dilute Nitrides*, edited by I. A. Buyanova and W. M. Chen (Taylor and Francis, New York, 2004).

⁴*Dilute Nitride Semiconductors*, edited by M. Henini (Elsevier, Amsterdam, 2005).

⁵T. D. Veal, L. F. J. Piper, S. Jollands, B. R. Bennett, P. H. Jefferson, P. A. Thomas, C. F. McConville, B. N. Murrin, L. Buckle, G. W. Smith, and T. Ashley, Appl. Phys. Lett. **87**, 132101 (2005).

⁶H. Naoi, Y. Naoi, and S. Sakai, Solid-State Electron. **41**, 319 (1997).

⁷D. K. Shih, H. H. Lin, L. W. Sung, T. Y. Chu, and T. R. Yang, Jpn. J. Appl. Phys., Part 1 **42**, 375 (2003).

⁸M. Kuroda, R. Katayama, S. Nishio, K. Onabe, and Y. Shiraki, Phys. Status Solidi C **0**, 2765 (2003).

⁹M. Kuroda, A. Nishikawa, R. Katayama, and K. Onabe, J. Cryst. Growth **278**, 254 (2005).

¹⁰T. S. Moss, Proc. Phys. Soc. B **67**, 775 (1954).

¹¹E. Burstein, Phys. Rev. **93**, 632 (1954).

¹²W. Walukiewicz, Appl. Phys. Lett. **54**, 2094 (1989).

¹³J. Tersoff, Phys. Rev. B **32**, 6968 (1985).

¹⁴J. Wu and W. Walukiewicz, Superlattices Microstruct. **34**, 63 (2003).

¹⁵E. P. O'Reilly, A. Lindsay, S. Tomic, and M. Kamal-Saadi, Semicond. Sci. Technol. **17**, 870 (2002), and references therein.

¹⁶A. Polimeni, M. Capizzi, M. Geddo, M. Fischer, M. Reinhardt, and A. Forchel, Appl. Phys. Lett. **77**, 2870 (2000).

¹⁷M.-A. Pinault and E. Tournié, Appl. Phys. Lett. **78**, 1562 (2001).

¹⁸Y. P. Varshni, Physica **34**, 149 (1967).

¹⁹I. Vurgaftman and J. R. Meyer, J. Appl. Phys. **94**, 3675 (2003).

²⁰A. Lindsay and E. P. O'Reilly (private communication).

²¹A. Lindsay and E. P. O'Reilly, Solid State Commun. **118**, 313 (2001).